Available online at www.sciencedirect.com
SCIENCE DIRECT®
ELSEVIER
Applied Energy 76 (2003) 449–466
APPLIED ENERGY
www.elsevier.com/locate/apenergy

Development of a numerical simulation system toward comprehensive assessments of urban warming countermeasures including their impacts upon the urban buildings' energy-demands

Yukihiro Kikegawa[a,*], Yutaka Genchi[b], Hiroshi Yoshikado[c], Hiroaki Kondo[d]

[a]*Global Environment Laboratory, Fuji Research Institute Corporation, 2-3 Kandanishiki-cho, Chiyoda-ku, Tokyo 101-8443 Japan*
[b]*Research Center for Life Cycle Assessment, National Institute of Advanced Industrial Science and Technology, 16-1 Onogawa, Tsukuba, Ibaraki 305-8569 Japan*
[c]*Research Center for Chemical Risk Management, National Institute of Advanced Industrial Science and Technology, 16-1 Onogawa, Tsukuba, Ibaraki 305-8569 Japan*
[d]*Institute for Environmental Management Technology, National Institute of Advanced Industrial Science and Technology, 16-1 Onogawa, Tsukuba, Ibaraki 305-8569 Japan*

Abstract

One of the detrimental effects caused by the urban warming phenomena is the increase of energy consumption due to the artificial air-conditioning of buildings in summer. In greater Tokyo, the temperature sensitivity of the peak electricity demand reaches up to 3%/°C in recent years, and about 1.5 GW of new demand is required as the daily maximum temperature increases by 1.0 °C. This huge demand for summer electricity is considered to be one of the common characteristics of big cities in Asian countries. In order to simulate this increase in cooling energy demands and to evaluate urban warming countermeasures from the viewpoint of buildings' energy savings, a numerical simulation system was developed adopting a new one-dimensional urban canopy meteorological model coupled with a simple sub-model for the building energy analysis. Then, the system was applied to the Ootemachi area, a central business district in Tokyo. Preliminary verification of the simulation system using observational data on the outdoor and indoor thermal conditions showed good results. Simulations also indicated that the cut-off of the anthropogenic heat from air-conditioning facilities could produce a

* Corresponding author. Tel.: +81-3-5281-5286; fax: +81-3-5281-5466.
E-mail address: kike@cyg.fuji-ric.co.jp (Y. Kikegawa).

0306-2619/03/$ - see front matter
doi:10.1016/S0306-2619(03)00009-6

cooling energy saving up to 6% with the outdoor air-temperature decrease by more than 1 °C in the summer urban canopy over Ootemachi area.

Keywords: Urban warming countermeasure; Anthropogenic heat; Urban canopy layer; Cooling energy conservation

1. Introduction

As a countermeasure against global warming, the reduction of the anthropogenic CO_2 emission's has become a concrete subject with numerical targets in the industrialized countries after the 3rd meeting of the Conference of the Parties to the United Nations Framework Convention on Climate Change (COP3), which was held in Kyoto in 1997. However, according to the domestic forecast, the energy consumption which has direct effect on the CO_2 emission will keep on increasing in the future in both commercial and residential sector's as well as transportation sector in our country [1]. Therefore, energy conservation in big cities, where the energy demand in these two sectors is concentrated is considered as one of the most important issues toward the CO_2 reduction in the future.

On the other hand, local warming—the so called as heat island phenomenon—is progressing in big cities in our country during the last centuries. For example in Tokyo, the temporal rate of this warming reaches up to 2 °C/100 year as for seasonal maximum air temperature in summer [2] and 4 °C/100 year as to averaged daily minimum temperature in winter [3]. Such increases of urban air temperature could result in increased cooling-energy consumption. This increase could create additional waste heat which may further intensify summer urban heat-islands. However, quantitative study has been hardly carried out on this vicious cycle problem. It is obvious that the investigation of this problem becomes extremely important if we recognize the huge increase of the peak electric-power demand of about 1.5 GW with 1 °C temperature rise in summer in the Tokyo metropolis [4].

Based on the above background, this study sets its goal as the establishment of a comprehensive assessment methodology for urban-warming countermeasures, which include the impacts of countermeasures upon urban energy demands. Toward this target, a numerical simulation system was developed, which can express the city-block-scale interaction between summertime outdoor thermal conditions and cooling-energy demands of buildings.

2. Simulation system

2.1. Framework of the system

Fig. 1 shows the composition of our developed simulation system. To analyze the physical relation between outdoor air conditions and cooling energy consumption of buildings in urban canopies, a numerical forecast of the meteorological fields around

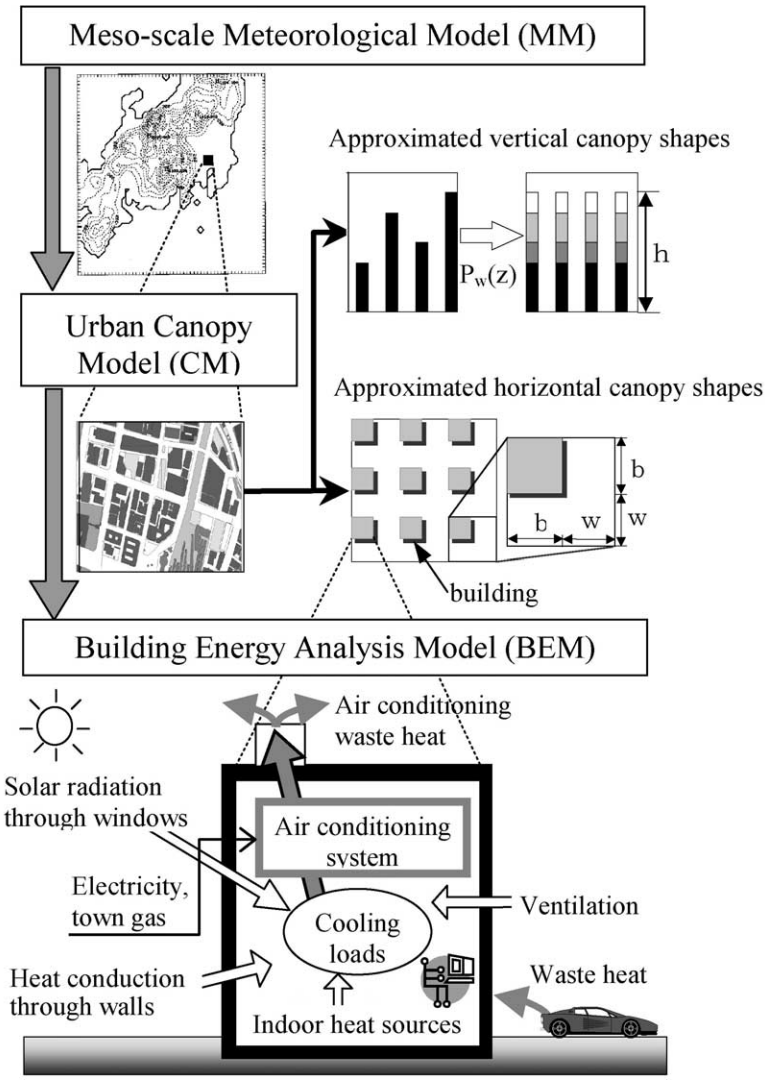

Fig. 1. Composition of the developed simulation system.

buildings was needed. Conventionally, meso-scale meteorological models have been often used for numerical studies on urban-warming phenomenon. However, the mesh size of these models usually reaches over 2 km horizontally. So, meso-scale models cannot explicitly take account of the physical influences of the urban canopies on the surface boundary layer over cities. What is represented in meso-scale models could be the open-space meteorological fields above urban canopies.

Therefore, we adopted our one-dimensional urban canopy model (CM) [5] for the city-block-scale meteorological forecast. Additionally, the larger-scale meteorological influences from outside of the urban canopy, i.e. local winds and upper

prevailing winds, etc. were introduced by a single direction connection of CM with our meso-scale meteorological model (MM) [6]. Moreover, in order to consider the architectural responses of air-conditioning energy consumption and its consequent waste-heat emission to the urban canopy meteorological conditions, the building energy analysis model (BEM) was developed [7].

Fig. 2 shows the computational flow of the simulation system that is composed of a MM, CM and BEM. Initial conditions and the upper boundary conditions of CM atmosphere were generated from the simulation results of MM. In this single direction coupling between CM and MM, the CM upper boundary was set to the altitude of the atmospheric mixing layer. The estimation of this altitude was based on the method of Kimura [8], in which temporal variation of mixing-layer depth was considered analytically. In addition to the above computation, BEM simulated the cooling load in the buildings (Q_c). BEM also computed the amount of cooling energy (E_c), which corresponded to the demanded energy for pumping out of Q_c from the building to keep the indoor temperature to the controlled one. In the calculation of E_c, the energy efficiency of the heat-pump equipment for cooling, which generally called as the coefficient of performance (COP), was also considered. Then, the air-conditioning waste-heat (Q_A) that is equivalent to the sum of Q_c and E_c was the output from the outdoor heat exchanger of heat-pump system to the CM atmosphere.

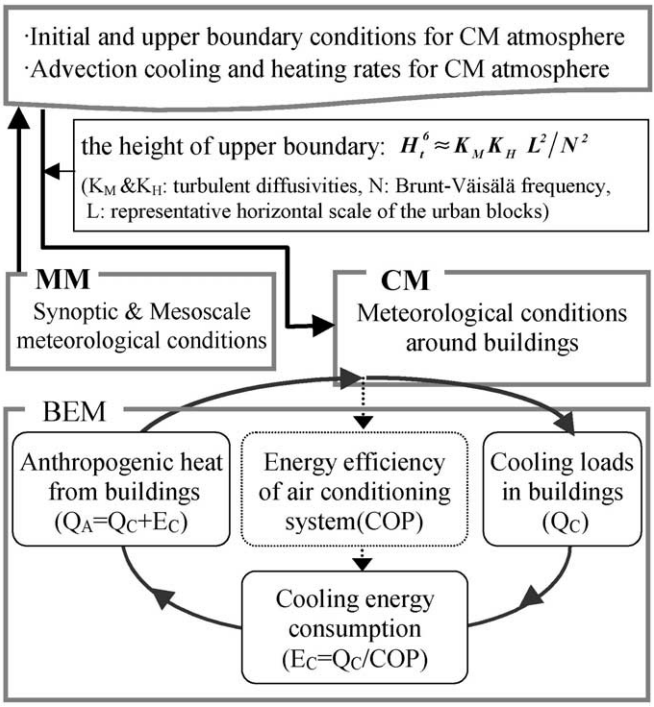

Fig. 2. Computational flow of the simulation system.

By this feedback of Q_A to the atmospheric heat balance in the urban canopy layer (UCL), CM and BEM were bi-directionally connected.

2.2. Details of submodels

CM is a vertical one-dimensional model, which can compute the temporal variations of air temperature, humidity and wind velocity in the UCL. CM takes into account the effects of building drag and anthropogenic heat release in the UCL. The effect of complicated radiation processes among the buildings were also considered, such as shading effect and reflection of short wave, and re-emission of long wave from building's and ground surfaces. CM considers an urban block of 0.5–1 km^2 in which buildings stand on a lattice array (Fig. 1). This horizontal arrangement of buildings is defined using two parameters. One is the average length of building's bottom (b), and the other is the average distance between buildings (w). As for vertical direction, the distribution of the height of buildings is considered. The floor density [$Pw(z)$] was introduced at each level in the urban canopy.

MM is a three-dimensional mesoscale meteorological model. Its computational domain covers about 600 km^2, and includes most of the central part of Japan (Fig. 1). Its horizontal grid spacing is about 10 km. Other details of CM and MM can be seen in Refs. [5,6]. Details of the newly developed BEM and its connection scheme with CM are described hereafter.

BEM is a box-type heat budget model in which a building in the urban block is treated as a box. In BEM, the cooling loads in the buildings are separately calculated for the sensible and the latent heat components. The following Eqs. (1) and (2) were used for the computation of the total sensible heat load H_{in} (W) and the total latent heat load E_{in} (W) in the building, respectively:

$$H_{in} = \sum_i A_i h_{ci}(T_{wi} - T_r) + \sum_j A_j \eta_j S_j + (1-\beta) C_p \rho V_a (T_a - T_r) + A_f q E + A_f P \varphi_p q_{hs}, \quad (1)$$

$$E_{in} = (1-\beta)\iota \rho V_a (q_{Va} - q_{Vr}) + A_f P \varphi_p q_{hl}. \quad (2)$$

Here, the subscripts i and j indicate the elements of the indoor surfaces of walls and windows respectively. A_i (m^2) and A_j (m^2) show those areas. The right-hand terms of Eq. (1) stand for components of the sensible heat load. The first term represents its heat exchange between walls and indoor air, and the second term the transmission of the solar insolation through the windows. The third term corresponds to the sensible heat exchange through ventilation. The fourth and last term's indicate the internal sensible heat generation from the equipment and occupants, respectively. As for the latent heat components, the water vapor intrusion through ventilation [the first right-hand term of Eq. (2)] and evaporation from occupants [the second right-hand term of Eq. (2)] are considered. The meanings of the other symbols in these equations are as follows: H_{ci} ($Wm^{-2}\,K^{-1}$): convective heat transfer coefficient; T_{wi} (K): indoor surface temperature of the walls, T_r (K): indoor air temperature; T_a (K): outdoor air tem-

perature computed by CM; η_j (–): insolation transmittance through the windows; S_j (Wm^{-2}): solar insolation on the windows computed by CM, β (–): thermal efficiency of the total heat exchanger; C_p ($Jkg^{-1}\ K^{-1}$): specific heat of air; ρ (kgm^{-3}): air density; V_a ($m^3\ s^{-1}$): total ventilation rate in the building; A_f (m^2): air-conditioned floor area; q_E (Wm^{-2}): sensible heat gain from equipments per floor area; P (person m^{-2}): peak number of occupants per floor area; φ_P (–): ratio of hourly occupants to P ($0 \leqslant \varphi_P \leqslant 1$); q_{hs} (W $person^{-1}$): sensible heat generation from the occupants, q_{hl} (W $person^{-1}$): latent heat generation from the occupants; ι ($J\ kg^{-1}$): latent heat of evaporation; q_{Va} ($kg\ kg^{-1}$): specific humidity of the outdoor air computed by CM; q_{Vr} ($kg\ kg^{-1}$): specific humidity of the room air. For the computation of T_{wi} in the BEM, the heat-balance equation on the indoor surface of the wall was solved in conjunction with the one-dimensional thermal conduction in the wall equation for each element of the indoor surfaces. Simultaneously, the heat budget on the outdoor surface of the wall was also considered in the CM.

The remaining unknown variables T_r and q_{Vr} were calculated by the following Eqs. (3) and (4):

$$Q_B \frac{dT_r}{dt} = H_{in} - H_{out}, \quad H_{out} = \varphi_p H_{in}, \tag{3}$$

$$\iota \rho V_B \frac{dq_{Vr}}{dt} = E_{in} - E_{out}, \quad E_{out} = \varphi_p E_{in}, \tag{4}$$

in which Q_B ($J\ K^{-1}$) and V_B (m^3) denote the overall heat capacity and the total volume of the indoor air in the building. H_{out} (W) and E_{out} (W) indicate the sensible and latent heat pumped out from the building for cooling, respectively. In Eqs. (3) and (4), the temporal variation rates of T_r and q_{vr} were formulated as to be proportional to the unprocessed heat loads [= the difference of the generated cooling loads (H_{in} and E_{in}) and the processed loads (H_{out} and E_{out})]. For the full air-conditioning occasion ($\varphi_p = 1$), a fixed control is assumed to be done where both T_r and q_{Vr} are fixed to the air-conditioning target values. Here, the influence of the thermal storage in the interior structures such as furniture and inner walls on the temperature variation of the room air was considered in some simplified manner [9], in which Q_B includes not only the heat capacity of the indoor air but also that of the interior structures. T_r and q_{vr} were also assumed to be uniform through the all air-conditioning space in the building.

The following Eqs. (5) and (6) were used for the calculation of the cooling energy consumption E_C (W) and its consequent waste-heat emission Q_A (W):

$$E_C = \frac{H_{out} + E_{out}}{COP}, \tag{5}$$

$$Q_A = E_C + (H_{out} + E_{out}) = \frac{COP + 1}{COP}(H_{out} + E_{out}). \tag{6}$$

COP here represents the energy efficiency of heat source equipment, and E_C indicates the energy usage for its operation. The operating power for auxiliary machinery such

as the cooling-water pump and supply fan was excluded from the computation. Considering the type of the heat-source equipment, air-cooled or water-cooled, Q_A was separately computed into the sensible heat (Q_{AS}) and the latent heat component (Q_{Al}).

As a prognostic equation for the atmospheric temperature in the CM, the following equation was used,

$$C_p\rho\frac{\partial\theta}{\partial t} = C_p\rho\frac{1}{m}\frac{\partial}{\partial z}\left(K_h m\frac{\partial\theta}{\partial z}\right) - C_p\rho\left(\alpha\vec{V}_M\right)\vec{\nabla}\theta_M + Q_{AS} + Q_{VS} \tag{7}$$

where θ (K) and K_h ($m^2\ s^{-1}$) indicate the atmospheric potential temperature and the vertical turbulent diffusion coefficient of sensible heat; and m (–) represents the effective volume ratio of the air in the urban canopy that is composed of the atmosphere and the buildings. On the right side of Eq. (7), the anthropogenic sensible heat (Q_{AS}) calculated by BEM was considered as a heat source term, along with another term which represents the sensible-heat exchange between the buildings and the atmosphere through ventilation (Q_{VS}). Moreover, the second right-hand term of Eq. (7), the cooling/heating rate due to the larger-scale atmospheric advection (such as land and sea breeze) outside the urban canopy, was introduced from the MM considering the wind velocity attenuation in the urban canopy. Here, V_M and θ_M are the wind velocity and potential temperature computed by the MM, and α is the attenuation factor of the wind velocity in the urban canopy, that is given as the ratio of the CM wind velocity against V_M. The same connection scheme of CM with BEM and MM as shown in Eq. (7) was also applied to the water-vapor transfer process in the CM.

The above-mentioned multi-scale simulation system is hereafter referred as the 'MM-CM-BEM'.

3. Verification of the simulation system

3.1. Measurement data

Simulations using MM-CM-BEM were conducted for the Ootemachi area, i.e. the central business district in Tokyo. The computational domain is a 500 m×500 m region (referred to as 'region-1') as shown in Fig. 3. The measurement data had been acquired in August, 1998 for a 25-story office building (i.e. 'Building O' hereafter) located at the center of the region-1, and was used for the verification of the MM-CM-BEM. Here, the measurement includes the continuous acquisition of meteorological data from the rooftop of Building O (approximately 100 m high). The data relating to its internal air-conditioning was also simultaneously collected. From the collected data such as hourly flow rate of chilled water and its temperature difference in cooling-use, it was possible to estimate the hourly amount of the actual cooling load generated in Building O.

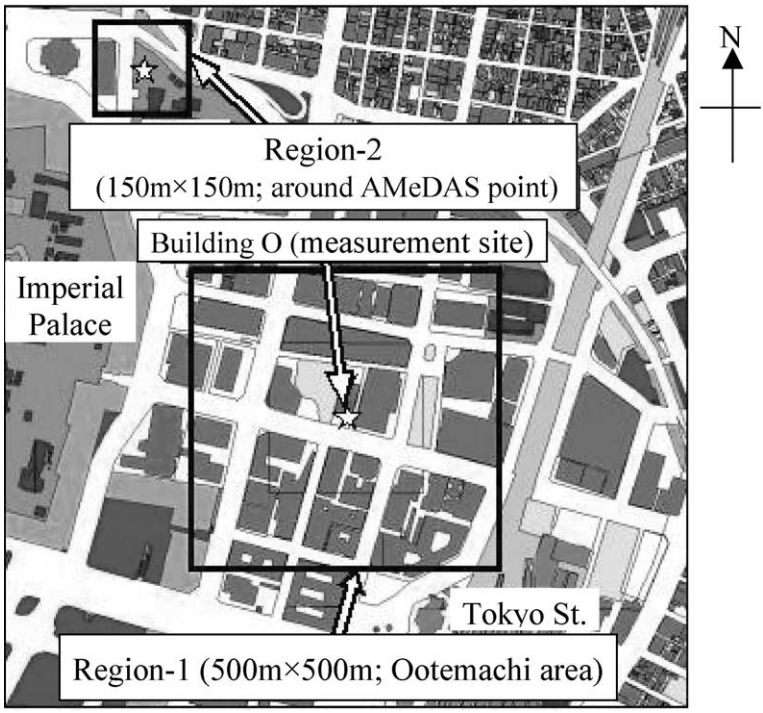

Fig. 3. Computational domain of CM-BEM.

3.2. Simulation conditions

As described in Section 2.2, the CM requires the parameters related with structures of the urban blocks for simulation. Those are b, w and $Pw(z)$. These parameters were derived from the GIS data [10] over region-1, where b and w were estimated to be 47 m and 23 m. $Pw(z)$ in which the regional averaged roof height corresponds to 45 m was also obtained.

As for the structures of the buildings, the parameters of typical office buildings was adopted for the widths and materials of walls, the coverage of windows, and thermal and radiative characteristics of the surfaces (Table 1). The external concrete walls was set to 22 cm in thickness with 5 cm internal insulation and expressed by equally divided 16 layers. The underground conditions are as follows: the concrete goes to 33 cm in depth, and the rest of the domain was the soil, up to 1.4 m depth for simulation. Refer to Table 1 for other assumptions concerning the canopy materials.

For air conditioning in the buildings, the typical conditions for office buildings were also adopted (Table 2). Considering the heat source composition in the district cooling system that was installed in the region-1, 70% of the heat-source equipment was assumed to be the town gas driven, absorption type hot and chilled water generator, which releases the latent waste heat from a cooling tower. The remaining 30% was assumed to be the electric air-source heat-pump which releases the sensible

Table 1
Parameters of the materials used in the calculation

	Surface albedo	Volumetric heat capacity ($J\ m^{-3}\ K^{-1}$)	Thermal conductivity ($J\ m^{-1}\ s^{-1}\ K^{-1}$)	Note
Underground (0–33 cm)	0.2 (0.15)	1.93×10^6	1.39	Concrete (with 10% of vegetation)
Underground (33–140 cm)	–	1.74×10^6	1.00	Soil
Roof materials (insulator)	–	0.06×10^6	0.04	Poly-ethylene foam
Roof materials (other parts)	0.2	1.93×10^6	1.39	Concrete
Wall materials (insulator)	–	0.06×10^6	0.04	Poly-ethylene foam
Wall materials (other parts)	0.2 (0.4)	1.93×10^6	1.39	Concrete (with 30% of window)

Table 2
Parameters of the air conditioning in the buildings used in the calculation

Parameters	Settings
Target temperature of room cooling	26.0 °C
Target relative-humidity of room cooling	50.0%
Ratio of air-conditioned floor area to total floor area	60%
Duration of air-conditioning on weekdays	0900–1800 LST[a]
Volumetric ventilation rate per unit floor area	5.0 $m^3\ m^{-2}\ h^{-1}$ [13]
Thermal efficiency of the total heat-exchanger (β)	60% [13]
Floor area per occupant	5.0 m^2 $person^{-1}$ [13]
Sensible heat generation from an occupant (q_{hs})	54.7 W $person^{-1}$ [13]
Latent heat generation from an occupant (q_{hl})	64.0 W $person^{-1}$ [13]
Insolation transmittance through the windows (η_j) (for windows with blinds)	30% [9]
Overall volumetric heat capacity of indoor air (Q_B) (including furniture and inner walls)	2.0×10^4 J m^{-3} K^{-1} [9]

[a] Pre-cooling starts from 0800 LST.

waste heat from the outdoor heat-exchangers. Its COP was estimated using the characteristic curve developed by Ashie [11], which showed the typical COP dependencies of air-source heat-pump systems to the partial load and the ambient air temperature. On the other hand, the COP of the absorption type hot and chilled water generator with less dependency upon those conditions was fixed at a value of 1.2. Other settings of the parameters, with temporal variations such as φ_P and q_E, etc. are shown in Fig. 4.

To obtain the initial and upper boundary conditions and the advection cooling/heating rates over the urban canopies in the region, a larger-scale meteorological simulation was conducted using MM. As for the anthropogenic waste heat, rough estimates of hourly values [12] for each MM horizontal grid were adopted. This simulation was initialized at 0000LST 2 August and terminated at 2400LST 5 August 1998. During this period, the computational domain of the MM was roughly under the Pacific Ocean anticyclone and the daily maximum temperature in Tokyo consecutively exceeded 32 °C under typical summer-day conditions. Using the results of the above MM computation, simulations by CM-BEM were carried out for the region during the same period. Here, a realistic setting was made for the

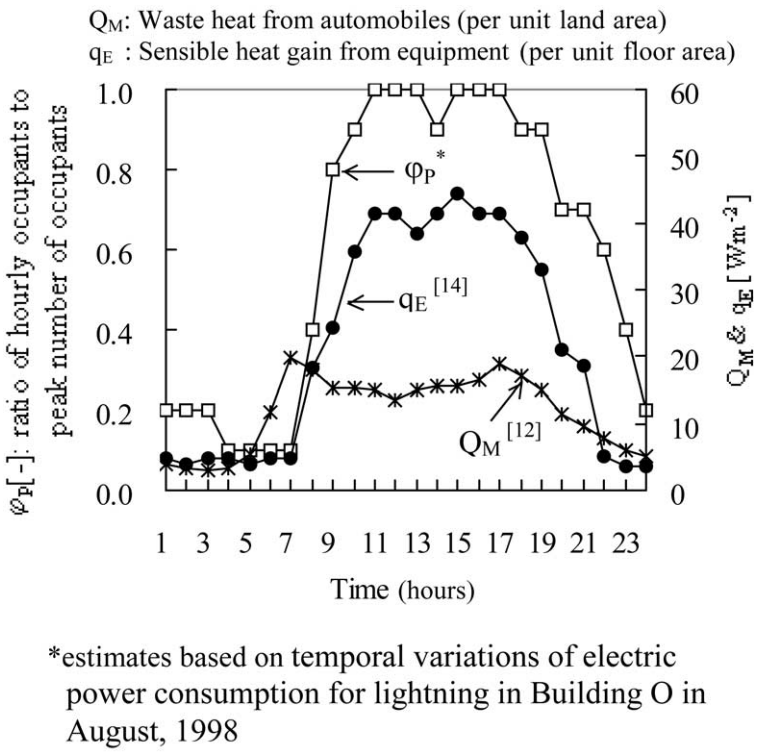

Fig. 4. Time-dependent parameters used in the calculation [12,14].

insolation condition by adopting the result of the solar radiation observation on the rooftop of Building O.

3.3. Comparison of simulation results and measurement data

The CM-BEM simulations were carried out under the assumptions for three cases, CASE-1-3 (Table 3), concerning the spatial placement of the waste heat sources of the buildings in the urban canopy.

Fig. 5 shows the comparison between computed and measured air temperature at the observation altitude (= 100 m) on the rooftop of Building O. The computational result of MM tends to slightly overestimate the amplitude of the temperature variation, and the remarkable difference (underestimation) from the measurement is recognized at night-time. This result is considered to be caused by the representing scheme of the urban canopy structure in the MM, where the urban canopy is simply treated as a uniform concrete plane because of its insufficient spatial resolution. In other words, the heat capacity of the urban canopy is underestimated, and the restraint process of nocturnal radiation cooling of the urban surfaces, which is caused by long wave re-emission from the buildings, is ignored in the MM. These problems

Table 3
Case settings in the simulation

Simulation case	Placements of the waste-heat sources of the buildings
CASE-1	Placed on the rooftop of each building
CASE-2	Placed near-ground around each building (at 3 m above the ground)
CASE-3	Placed somewhere not exposed to the atmosphere (waste heat was assumed to be released not into the atmosphere but elsewhere such as into sewage or soil)

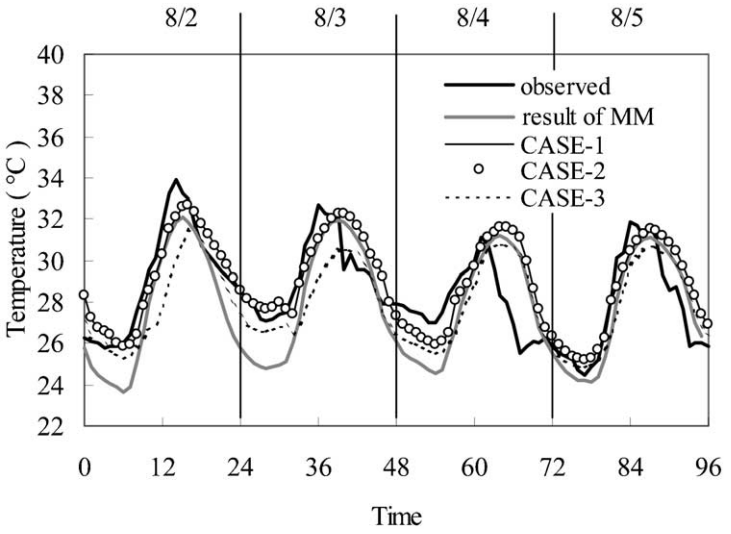

Fig. 5. Computed and measured air temperature at the observation altitude (=100 m) on the rooftop of Building O in region-1.

are considered to be the causes of the inadequate reproducibility of the air temperature in the MM. On the contrary, the CM-BEM which takes into account these effects of canopies is able to approximately reproduce the daily variation of air temperature, including during the night-time as shown in Fig. 5. In the daytime, the results of CASE-1 (anthropogenic heat discharge from rooftop) and CASE-2 (anthropogenic heat discharge from near-ground) show better correspondence with the observations compared to that of CASE-3 in which the anthropogenic heat from the building is fully cut off. These results are reasonable, because a lot of heat exchangers of air-conditioning systems actually exist mainly on the rooftop of each building in the region. The amplitude of the air temperature increase caused by the anthropogenic heat among cases (CASE-1-3) was about 1 °C in the daily averages through the simulation period. Excluding the insufficient reproduction of the rapid drop in the measured air temperature that was seen in the afternoon of August 3 and 4, CM-BEM manifested more realistic reproducibility of the air temperature in the

upper part of the urban canopy than MM did. This rapid temperature drop was due to a temporary soothing of the seasonal rain front. The MM-CM-BEM was not completely able to reproduce the change of the local wind caused by this front moving over Tokyo, and as a result, the air temperature was overestimated. Inaccuracies of the initial and boundary conditions, given the large computational domain of MM, may be the cause of this problem.

Fig. 6 shows the comparison between computed and observed near-ground air temperature. The observed data were acquired by AMeDAS (Automated Meteorological Data Acquisition System) of the Meteorological Agency at a location approximately 700 m northwest of Building O. For the computation of the air temperature near the bottom of the urban canopy, the geometrical parameters for the local canopy structure, i.e. b, w and $Pw(z)$, were redefined using GIS data over 150 m×150 m region around the observation point (region-2 in Fig. 3). The green coverage on the ground surface was also modified to 40% for this region based upon the aerial photo-interpretation. Other conditions were assumed to be the same as those for region 1. As in the case for the region 1, CM-BEM (CASE-1 and -2 in Fig. 6) reproduced the daily course of the air temperature more realistically in the lower part of the urban canopy than MM did. Here, the reason for the differences of the computational results from the AMeDAS temperature in the afternoon of August 3 and 4 is the same as in the case of Fig. 5.

In Fig. 7, the comparisons of the actual measurements and predicted results by CM-BEM are shown concerning the average room-air temperature and the amount of the processed cooling loads in Building O, which correspond to the sum of H_{out} and E_{out} in Eqs. (3) and (4). The computed room temperature and processed cooling loads were approximately consistent with each actual measurement. The underestimation

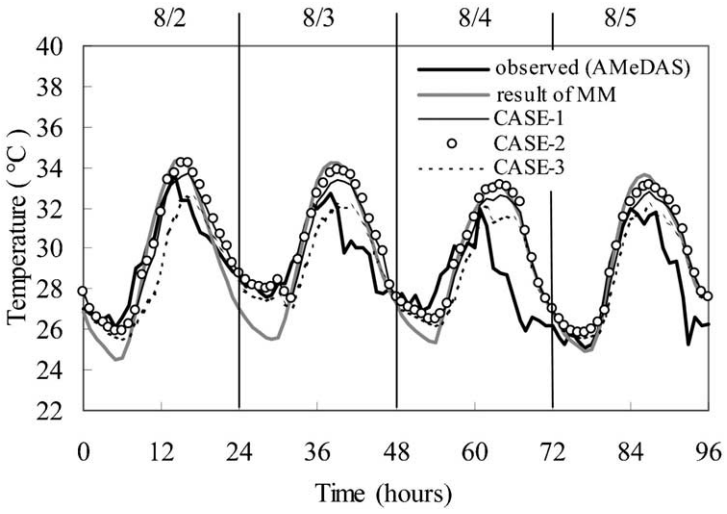

Fig. 6. Computed and observed near-ground air temperature in region-2. The observed one was acquired at an AMeDAS point which was located 700 m northwest of Building O.

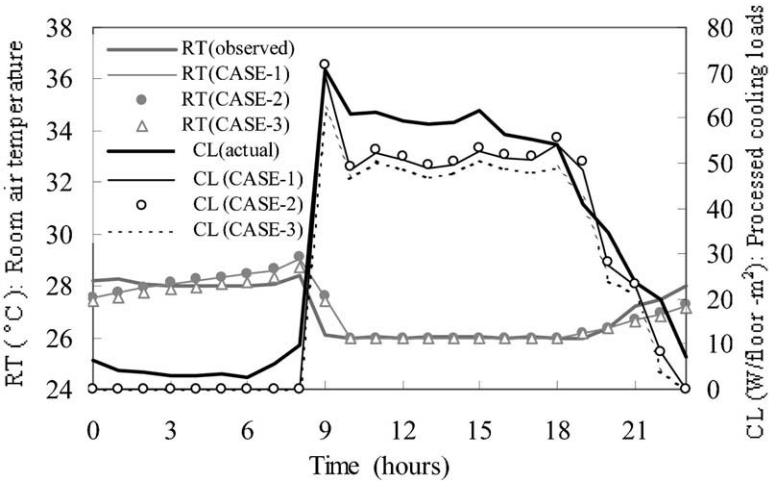

Fig. 7. Comparisons of the actual measurements and calculation results by CM-BEM in region-1 concerning the average room air temperature (RT) and the amount of the processed cooling loads (CL) in Building O.

of about 10 W/m^2 (20%) for the diurnal processed cooling loads is caused by the settings for heat gain rate from the equipment (q_E in Fig. 4), which occurs for the majority of total cooling loads.

In the above-mentioned simulations, the vertically integrated value of the anthropogenic heat computed by CM-BEM in CASE-1 and -2 reached 450 W/m^2 (per land area) during daytime for the region-1, and the ratio of the sensible heat to the latent heat was 1.0:2.2. The contribution of the car to the sensible anthropogenic heat peaked at 12%, and the building's waste-heat was predominant.

The computational results shown in Figs. 5–7 made clear that CM-BEM was capable of roughly reproducing the temporal variations of the outdoor air temperature and the indoor thermal environment in the summer urban canopy.

4. Discussion

4.1. Reproducibility of temperature sensitivity of regional electricity demand

Fig. 8 is a comparison between the daily maximum regional electric power demands and the daily maximum near-ground air temperature in the central districts of Tokyo during the weekdays from June to August 1998. Here, the former electricity demands were measured by a branch office of the Tokyo Electric Power Company (referred to as 'branch office A' hereafter), which is in charge of the whole central business district of Tokyo, including the Ootemachi area, while the latter air temperature was obtained at the AMeDAS station located near the Ootemachi district (Fig. 3). A temperature sensitivity of the daily maximum electricity demand was estimated by regression analysis for the days whose maximum temperature exceeds

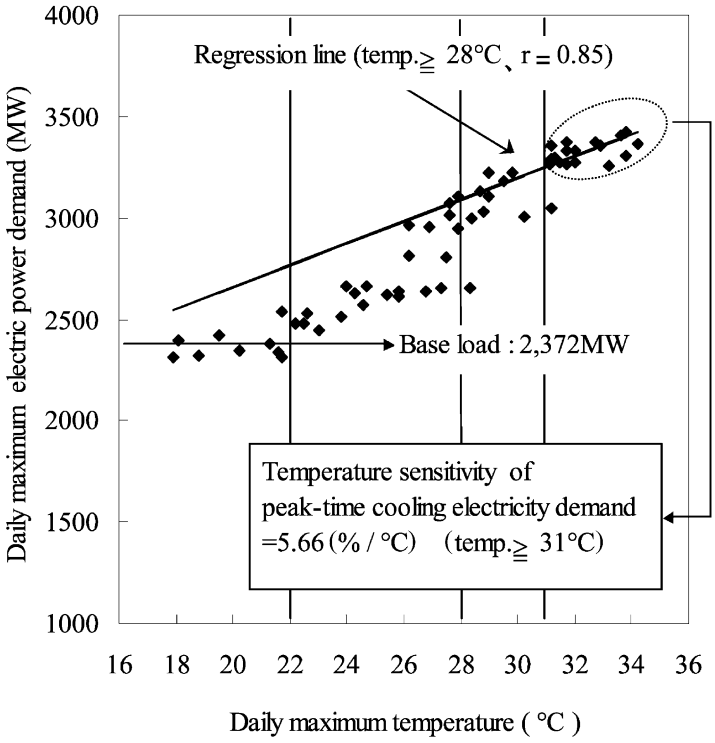

Fig. 8. Relation between the daily maximum regional electric-power demands and the daily maximum near-ground air temperature in the central districts of Tokyo during weekdays from June to August 1998. The electricity demands were measured by a branch office of the Tokyo Electric Power Company.

28 °C when most cooling systems were considered to be in operation. Consequently, the estimated sensitivity of 53.75 MW/°C (correlation coefficient = 0.85) was obtained. This value was considered to be a peak-time demand increment of cooling electricity per unit air temperature rise by 1 °C. Next, this increment was compared with the total peak-time demands of cooling electricity. Here, the latter demands were estimated for each day by subtracting a base electricity-demand, excluding cooling usage, from the daily maximum demands plotted in Fig. 8. The base demand was assumed to be 2372 MW as the average value of the daily maximum demands during the days whose daily maximum temperature were less than 22 °C. Then, the ratios of the above-mentioned sensitivity (53.75 MW/°C) to the daily peak-time demands of cooling electricity were calculated, and 5.66%/°C was obtained as the average ratio for the days whose daily maximum temperature exceeds 31 °C. This result means that the peak-time demand of cooling electricity increases by 5.66% with 1 °C air temperature rise in the electricity-supply region of branch office A. The reason for selecting a threshold of 31 °C for the daily maximum temperature here was to consider the consistency with the range of the computed air-temperature in region 1 (Fig. 5). Although the cooling electricity demands in this analysis include

the operating power for the air-conditioning auxiliary machinery, its dependency on the outdoor-air temperature could be negligible [11]. Therefore, the above-mentioned sensitivity (= 5.66%/°C) can be regarded as the regional-average temperature sensitivity of the peak-power demand of heat-source equipment in the buildings.

On the other hand, Fig. 9 is a comparison of the computational results for CASE-1–3 by CM-BEM in region 1 between the daily maximum surface-air temperature and the daily maximum cooling electricity demands, which correspond to the maximum power needed for the heat-source equipment. Both were in a clear linear relation, and we obtained a sensitivity of 6.07%/°C that was approximately consistent with the actual value (= 5.66%/°C) estimated in the branch office of A region. This result also validates the CM-BEM.

4.2. Impact of anthropogenic heat distribution on cooling energy-demands

Table 4 shows comparisons between the computed daily totals of the cooling electricity and town-gas demands and the daily average surface-air temperature in region 1. CASE-1 is chosen as the control-run here. The down shifts of waste heat sources of the buildings from their rooftops to the ground levels (CASE-1→2) increase the daily average surface-air temperature by 0.62 °C. On the other hand, the cut-off of waste heat from the buildings (CASE-1→3) resulted in the temperature

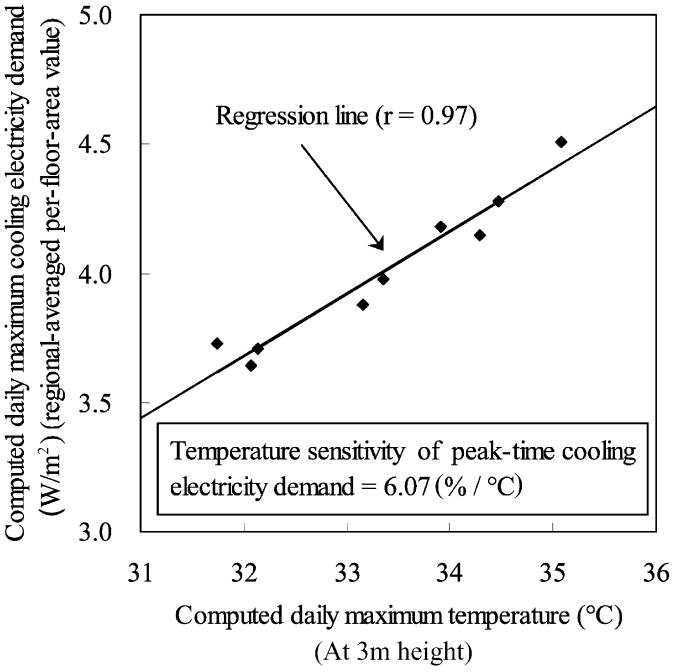

Fig. 9. Comparison of the computational results on CASE-1-3 by CM-BEM in region-1 between the daily maximum surface-air temperature and the daily maximum cooling-electricity demands.

Table 4
Comparisons of the computed daily totals of the cooling-electricity and town-gas demands and the daily average surface-air temperature in region obtained through the CM-BEM simulation

Simulation cases	Daily total cooling energy demands per unit floor area (regional averaged values) J m^{-2} day^{-1})				Daily average air temperature (At height 3m)	
	Town gas	Electricity	Total	Percent change	(°C)	Differences (°C)
CASE-1	1358.23	174.86	1533.09	(control)	30.37	(control)
CASE-2	1386.88	189.02	1575.90	+2.79	30.99	+0.62
CASE-3	1284.27	159.71	1443.98	−5.81	29.08	−1.28

drop by 1.28 °C. Correspondingly, the daily totals of the cooling energy demands, which are the sums of the cooling-electricity and town-gas demands, increased by 2.79% (CASE-1→2) and decreased by 5.81% (CASE-1→3), respectively. The latter energy saving was caused by about a 6% reduction of the cooling load in the buildings, which resulted from the air-temperature drop by 1.28°C. This reduction in the cooling load was mainly caused by the decrease in heat gain through ventilation. The actual placements of the waste-heat sources in region 1 are the most realistically represented on CASE-1 (rooftop placements) among the cases. Therefore, the above mentioned results indicate a possible range of the urban warming mitigation and its consequent energy saving produced by the control of the anthropogenic heat release in the summer urban canopy over densely urbanized area in central Tokyo. As a concrete measure of this anthropogenic heat control, we have been proposed the introduction of the regional heating and cooling system using a ground-source heat pump [15], which sequesters waste-heat underground by using the soil as heat sink in summer.

5. Conclusions

From the viewpoint of urban energy-conservation, we developed a numerical simulation system that can express the city-block-scale interaction between summertime outdoor thermal-conditions and cooling energy demands in the urban canopies.

Then, the simulation system was applied to the Ootemachi area, a central business district in Tokyo. Simulations indicated that the system could reasonably reproduce the temporal variations of the outdoor-air temperature and the indoor thermal environment in the Ootemachi canopies under summer-day conditions. The simulated temperature sensitivity (6.07%/°C) of the peak-time cooling electric power demand in the Ootemachi area was almost consistent with the actual regional-average sensitivity (5.66%/°C) over all business districts in the central part of Tokyo, which was estimated using actual electricity-demand data provided by the Tokyo Electric Power Company. Next, the impacts of the air-conditioning waste heat source upon the outdoor air-temperature and cooling-energy demand were investigated using simulation results. Then, the near-ground air-temperature dropped by

more than 1 °C and about 6% of cooling energy consumption could be reduced by the cut-off of all air-conditioning waste-heat in the Otemachi urban canopy.

Finally, the applicability to summer business districts of our simulation system was confirmed. In the near future, we intend to apply the simulation system to urban districts with different conditions such as a residential area, and to expand its applicability to winter urban canopies. We are also planning to improve our system so as to be applicable to year-round evaluations of urban warming countermeasures from the viewpoint of urban energy-conservation to stop the increase in anthropogenic CO_2 emissions.

Acknowledgements

This study was supported by the Proposal-Based New Industry Creative Type Technology R&D Promotion Program from the New Energy and Industrial Technology Development Organization (NEDO) of Japan. We wish to express our gratitude to Tokyo Electric Power Company for their kind contribution of valuable data concerning the electric-power demand.

References

[1] Agency of Natural Resources and Energy. Demand and supply commission progress report, 1998 [in Japanese].
[2] Fujibe F. An increasing trend of extremely hot days in the inland of the Kanto Plain and its relation to urban effects. Tenki 1998;45(8):643–53 [in Japanese].
[3] Fujibe F. Long-term change of extreme temperature at urban meteorological stations in Japan. Tenki 1997;44(2):101–12 [in Japanese].
[4] Tokyo Electric Power Company. TEPCO illustrated, 1998 [in Japanese].
[5] Kondo H, Liu H. A study on the urban thermal environment obtained through one-dimensional urban canopy model. Journal of Japan Society for Atmospheric Environment 1998;33(3):179–92 [in Japanese].
[6] Kondo H. The thermally-induced local wind and surface inversion over the Kanto Plain on calm winter nights. Journal of Applied Meteorology 1995;34(6):1439–48.
[7] Kikegawa Y, Kondo H, Yoshikado H. A study on the dynamical interaction between thermal environment and building energy consumption in the urban canopy. In: Proceedings of 15th International Congress of Biometeorology & International Conference on Urban Climatology, Sydney, 1999.
[8] Kimura R. Dynamics of steady convections over heat and cool islands. Journal of the Meteorological Society of Japan 1975;53(6):440–57.
[9] Shukuya M. Radiative and thermal environment engineering in architecture. Maruzen, 1993 [in Japanese].
[10] Tokyo Metropolitan Government Bureau of Urban Planning. Land-use of Tokyo, 1998 [in Japanese].
[11] Ashie Y, Tanaka M, Yamamoto T. Heat discharge characteristics of air-conditioning systems of office buildings. Transactions of the Society of Heating, Air-Conditioning and Sanitary Engineers of Japan 1999;75:89–97 [in Japanese].
[12] National Institute for Resources and Environment. Development of assessment methodology of summertime countermeasures against urban heat-islands in big cities. Study report of Environmental Assessment Department, no. 97-1, 1997 [in Japanese].
[13] Inoue U. Handbook for air-conditioning. Maruzen, 1996 [in Japanese].

[14] Ojima-toshio Laboratory. Consumption rates of electric power and demanded energy for air-conditioning and hot-water supply in buildings. Tokyo: Waseda University Press; 1995 [in Japanese].
[15] Genchi Y, Kondo H, Kikegawa Y, Komiyama H. Feasibility of a regional-scale heat supply and air-conditioning system using a ground source heat-pump around the Nishi-Shinjuku area and its effect on reducing anthropogenic heat in summer. Energy and Resources 1999;20(6):562–9 [in Japanese].